Performance of SPAD-Detector in The Presence of Atmospheric Turbulence

Abdulmajeed Alanazi
Electrical and Electronic Engineering
The University of Manchester
Manchester, United Kingdom
abdulmajeed.alanazi@postgrad.manchester.ac.uk

Khairi Hamdi
Electrical and Electronic Engineering
The University of Manchester
Manchester, United Kingdom
K.Hamdi@manchester.ac.uk

***Abstract*—In this paper, a novel and accurate expression for the Bit Error Rate (BER) has been developed. Additionally, the performance of a free-space optical (FSO) communication system based on a direct-detection single photon avalanche diode (SPAD) array is examined, demonstrating higher sensitivity compared to traditional photodiodes. The impact of SPAD dead time is presented. On-Off Keying (OOK) modulation is employed, given its popularity in FSO systems due to its simplicity and cost-effectiveness. Two scenarios are explored: weak turbulence conditions and the saturation region turbulence. The weak turbulence channel is modeled using the log-normal channel model, while the saturation region turbulence channel is represented by the negative exponential channel model. The accuracy of the derived expression is validated through Monte-Carlo simulation. The results from both simulation and approximation illustrate how the atmospheric channel is affected by turbulence, specifically the eddies formed due to variations in refractive index resulting from temperature fluctuations, leading to an increased Bit Error Rate (BER).**

***Index Terms*—Single Photon Avalanch Diode (SPAD), Photon counting, atmospheric turbulence, on-off keying (OOK).**

I. Introduction

In recent years, researchers and academics have turned their attention to Free-Space-Optics (FSO) communication technology instead of the conventional radio-frequency (RF) approach, recognizing its effectiveness. FSO links possess an exceptionally high optical bandwidth in comparison to RF, enabling significantly higher data rates. These FSO systems are employed over long distances to facilitate high-rate communication [1]. Free-Space-Optics (FSO) communication links face challenges due to atmospheric turbulence, resulting in irradiance fluctuations in the received signal. This phenomenon, known as scintillation, induces fading and adversely affects the performance of FSO systems, leading to an increase in the Bit Error Rate (BER). In [2] various communication techniques have been outlined to address intensity fluctuations induced by turbulence in Free-Space-Optics (FSO) systems. Another challenge encountered by FSO systems is pointing error, impacting the Line-of-Sight (LOS) between the transmitter and receiver. This issue can be attributed to atmospheric deviations causing variations in the transmitted beam, resulting in communication interruptions and degradation in system performance [3]. Avalanche photodiodes (APDs) are commonly employed as receivers in Free-Space-Optics (FSO) systems. However, their performance is deemed unsatisfactory due to the inclusion of transimpedance amplifiers (TIAs), which substantially diminishes receiver sensitivity and restricts the signal-to-noise ratio (SNR). Consequently, single photon avalanche diodes (SPADs) emerge as a more suitable receiver alternative, as they eliminate the need for transimpedance amplifiers (TIAs). The utilization of SPAD receivers allows for significantly higher sensitivity and optical power efficiency compared to APDs [4]. A single SPAD receiver is limited by its ability to detect only one photon within a specific dead time unique to the device. This constraint poses a challenge in recovering signals, as the SPAD diode can register only one photon within a designated time frame. Consequently, if the time extends beyond this period, the photon may go undetected [5]. A Single Photon Avalanche Diode (SPAD) experiences dead time, a consequence of the quenching process that occurs after each photon detection event. This quenching process introduces a finite recovery time, commonly referred to as dead time [6]. This paper explores the utilization of a Single Photon Avalanche Diode (SPAD) array to address the dead time effect, aiming to enhance photon counting capabilities and overall performance.

In reference [8], the authors have introduced a novel photodetection receiver for Free Space Optics (FSO). They conducted a comprehensive investigation of the proposed detector, focusing on parameters such as dead time, counting probability, and effective count rate. Their analysis delves into system performance under On-Off Keying (OOK) modulation, specifically examining Bit Error Rate (BER). However, it's worth noting that they employed a Gaussian noise approximation for the channel without considering atmospheric turbulence modeling, a crucial factor in BER evaluation. To address this gap, our work represents the first attempt to study log-normal and negative exponential-based atmospheric channel effects in the context of OOK in FSO. Our contribution involves developing an analytical model for OOK under these turbulence models, evaluating BER, and conducting performance analysis through Monte Carlo simulations in MATLAB. Additionally, we compare the analytical, simulation, and approximation results to ensure coherence in the underlying assumptions.

979-8-3503-7099-7/24/$31.00 ©2024 IEEE

II. SYSTEM MODEL

Fig. 1 illustrates the block diagram of free-space optical communication, utilizing the atmosphere as a guided medium for transmitting optically modulated information signals. Through various electrical-to-optical and optical-to-electrical circuits, optical wireless systems transmit user information via optical modulation, which is then converted into the electrical domain at the receiver. FSO systems offer high data rates, leveraging transmission mechanisms akin to light-wave technology.

An optical laser is employed to transmit optical power through the channel, using a LASER to transmit optical power over the FSO channel. The atmospheric channel experiences turbulence, manifested as eddies resulting from variations in refractive index due to temperature fluctuations. The choice of modulation techniques significantly influences the connection quality between the transmitter and receiver in any communication system. Among various options, On–Off Keying (OOK) stands out as the most popular in FSO systems due to its simplicity and cost-effectiveness.

In our work, we consider weak turbulent conditions and saturation region turbulence. OOK is deemed suitable in these scenarios, although it may not be optimal for strong turbulent conditions. The SPAD detector is chosen over other common photodetectors like PIN and APD due to its higher sensitivity. Our weak turbulence channel is modeled using the log-normal channel model, and the saturation region turbulence channel is modeled using the negative exponential channel model. Further details on the FSO channel model and SPAD receiver are explained in the following subsections.

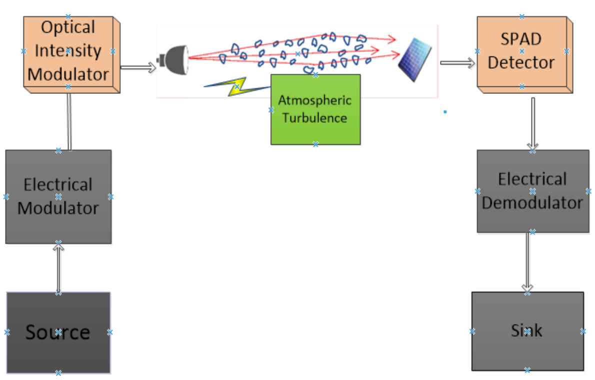

Fig. 1. *System Model of FSO*

In this work, we utilize a Single Photon Avalanche Diode (SPAD) detector. The details of this choice are described in the subsequent subsection outlined below.

A. *SPAD Detector Noise Evaluation*

The photocount statistic varies depending on the SPAD dead time. In the absence of SPAD dead time, the detection of photon arrival events can be modeled as a Poisson distribution.

- λ represents the average photon arrival rate, and it is related to the power of the optical signal as per reference [7]:

$$\lambda = \frac{\eta_{\mathrm{QE}} P_{\mathrm{s}}}{h\nu}, \tag{1}$$

Here, η_{QE} epresents the quantum efficiency of the SPAD, P_{s} denotes the power of the incident optical signal, h is the Planck's constant and ν represents the frequency of the optical signal. Contrarily, when considering SPAD dead time, the photon arrival statistics no longer follow a Poisson distribution. Therefore, the Probability Mass Function (PMF) of detecting k photons during the time interval $[0,\ T_{\mathrm{b}})$ is given by [8]:

$$p_K(k)=\begin{cases} \sum_{i=0}^{k}\psi(i,\ \lambda_k)-\sum_{i=0}^{k-1}\psi(i,\ \lambda_{k-1}) & k<k_{\max} \\ 1-\sum_{i=0}^{k-1}\psi(i,\ \lambda_{k-1}) & k=k_{\max} \\ 0 & k>k_{\max} \end{cases} \tag{2}$$

where $\lambda_k=\lambda(T_{\mathrm{b}}-k\tau),\ \lambda_{k-1}=\lambda(T_{\mathrm{b}}-(k-1)\tau)$ and the function $\psi(i,\lambda)$ is defined as:

$$\psi(i,\ \lambda)=\frac{\lambda^i e^{-\lambda}}{i!}.$$

and the maximum observable count during this period is $k_{\max}=\lfloor\delta\rfloor+1$

The mean and variance of photocount distribution in (2) are:

$$\mu_K = k_{\max} - \sum_{k=0}^{k_{\max}-1}\sum_{i=0}^{k}\psi(i,\ \lambda_k), \tag{3}$$

$$\sigma_K^2=\sum_{k=0}^{k_{\max}-1}\sum_{i=0}^{k}(2k_{\max}-2k-1)\psi(i,\ \lambda_k) - \left(\sum_{k=0}^{k_{\max}-1}\sum_{i=0}^{k}\psi(i,\ \lambda_k)\right)^2. \tag{4}$$

In this paper, an SPAD array is employed to enhance the performance of the receiver, particularly the photocount capacity, and mitigate the dead time effect. Therefore, the Probability Mass Function (PMF) in (2) can be rearranged for the mnth element of the array as $p_K(k_{mn})$ with parameters accounting for dead time and the impact of FF. The Fill Factor (FF) is defined as the ratio of the SPAD array's total active area to the total array area. It represents the probability of photons hitting the active area.

$$k_{\max,mn}=\left\lfloor\frac{T_{\mathrm{b}}}{\tau_{mn}}\right\rfloor+1,$$
$$\lambda'_{k_{mn}}=C_{\mathrm{FF}}\lambda_{mn}(T_{\mathrm{b}}-k_{mn}\tau_{mn}),$$

Here, λ_{mn} is the average photon arrival rate at the mnth SPAD, and τ_{mn} is the dead time of the mnth element. In general, obtaining a closed-form solution for an SPAD array detector is challenging, especially when the number of array elements is large. Here, X is the random variable representing the sum of elements of the SPAD array, where each element individually follows a Poisson random distribution of K. This can be mathematically represented as $X=\sum k$. According to the Central Limit Theorem (CLT), the counting distribution of the SPAD array can be approximated by a Gaussian distribution:

$$p_X(x) \sim N(\mu_X,\ \sigma_X^2), \tag{5}$$

The mean (μ_{mn}) and variance (σ_{mn}^2) of the photocount distribution of the mnth SPAD in the array:

$$\mu_X = \sum_{m=1}^{R}\sum_{n=1}^{C}\mu_{mn},$$
$$\sigma_X^2 = \sum_{m=1}^{R}\sum_{n=1}^{C}\sigma_{mn}^2.$$

III. BER EVALUATION OF OOK OVER ATMOSPHERIC TURBULENCE

A. Log-Normal Channel

In this study, under weak turbulence conditions (clear air turbulence), the intensity of the optical field can be accurately modeled using a random variable with a probability density function (pdf) that follows that of a log-normal random variable. So, if ζ denotes the intensity of the received optical field, then:

$$f(\zeta) = \frac{1}{\sqrt{2\pi\sigma_i^2}\zeta}\exp\left(-\frac{(\ln(\zeta)-m_i)^2}{2\sigma_i^2}\right), \quad i \geq 0 \tag{6}$$

The received signal is:

$$y = \zeta x_t + n(t) \tag{7}$$

where in (1) P_{s} is received optical power, hence:

$$P_{\mathrm{s}} = \zeta x_t \tag{8}$$

In this scenario, λ_k will change as a function of λ, where λ is a function of P_{s} representing the fading channel, which could be log-normal or negative exponential.

The performance of the SPAD receiver is influenced by factors such as dead time, dark count rate (DCR), afterpulsing, and crosstalk. This study investigates the effects on the performance of the SPAD receiver and provides the probability of error for On-Off Keying (OOK) modulation over a log-normal distribution. The system transmits at the bit rate $R_{\mathrm{b}} = 1/T_{\mathrm{b}}$, where T_{b} is the slot duration.

The average number of photons hit on each single SPAD per bit time interval is K_{n} when "0" bit is transmitted, and $K_{\mathrm{s}} + K_{\mathrm{n}}$ when a "1" bit is transmitted. where K_{s} denoted as contribution to the average count from the signal and K_{n} is background noise counts per bit interval T_{b} for each array element. So, $K_{\mathrm{s}} = \lambda_{\mathrm{s}}T_{\mathrm{b}}$ and $K_{\mathrm{n}} = \lambda_{\mathrm{n}}T_{\mathrm{b}}$, where λ_{s} and λ_{n} are assuming as the average photon arrival rate from source and background noise, respectively. The probability of x photons when "0" or "1" are sent, are given by:

$$\begin{aligned} p_0(x) &= p_X(x;\lambda_{\mathrm{n}}),\\ p_1(x) &= p_X(x;\lambda_{\mathrm{s}}+\lambda_{\mathrm{n}}). \end{aligned} \tag{9}$$

The Gaussian approximation in (5) can be applied to $p_0(x)$ and $p_1(x)$ so that $p_0(x) \sim \mathcal{N}(\mu_0, \sigma_0^2)$ and $p_1(x) \sim \mathcal{N}(\mu_1, \sigma_1^2)$. Therefore, the conditional probability of error P_e given ζ can be expressed as:

$$P_{e|\zeta} = Q\left(\frac{\mu_1(\zeta)-\mu_0}{\sigma_1(\zeta)+\sigma_0}\right). \tag{10}$$

The average probability of error can be expressed as:

$$P_e = \int_0^\infty Q\left(\frac{\mu_1(\zeta)-\mu_0}{\sigma_1(\zeta)+\sigma_0}\right) f(\zeta) d\zeta \tag{11}$$

This expression usually does not lead to a tractable result. Hence, using (6), (11) to drive the unconditional Bit Error Rate (BER) expression is given by:

$$\begin{aligned} P_e = &\frac{1}{\sqrt{2\pi\sigma_i^2}\zeta}\int_0^\infty Q\left(\frac{\mu_1(\zeta)-\mu_0}{\sigma_1(\zeta)+\sigma_0}\right)\frac{1}{\zeta}\\ &\exp\left(-\frac{(\ln(\zeta)-m_i)^2}{2\sigma_i^2}\right) d\zeta \end{aligned} \tag{12}$$

Making the change of variable $x = (\ln(\zeta) - m_i)/\sqrt{2}\sigma_i$

We then have

$$P_e = \frac{1}{\sqrt{\pi}}\int_{-\infty}^\infty Q\left(\frac{\mu_1(\zeta)-\mu_0}{\sigma_1(\zeta)+\sigma_0}\right) e^{-x^2} dx \tag{13}$$

Using the approximation

$$\begin{aligned} P_e &= \frac{1}{\sqrt{\pi}}\int_{-\infty}^\infty Q\left(\frac{\mu_1(e^{\sqrt{2}\sigma_k x_i + m_k})-\mu_0}{\sigma_1(e^{\sqrt{2}\sigma_k x_i + m_k})+\sigma_0}\right) e^{-x^2} dx\\ &\approx \sum_{i=-N; i\neq 0}^{N} w_i g(x_i) \end{aligned} \tag{14}$$

after the simplifying is given:

$$P_e \approx \frac{1}{\sqrt{\pi}}\sum_{i=-N; i\neq 0}^{N} w_i Q\left(\frac{\mu_1(e^{\sqrt{2}\sigma_k x_i + m_k})-\mu_0}{\sigma_1(e^{\sqrt{2}\sigma_k x_i + m_k})+\sigma_0}\right) \tag{15}$$

where $\{w_i\}$ and $\{x_i\}(i = -N, -N+1, \ldots -1, 1, 2, \ldots, N)$ are the weight factors and the zeros of the Hermite polynomial, respectively [9].

B. Negative Exponential Channel

In the limit of strong turbulence (i.e., during the saturation regime and beyond), the negative exponential model channel is widely accepted [10]. Also, the negative exponential pdf can be used when large propagation distances are considered, as given by:

$$f(\zeta) = \frac{1}{\gamma}\exp\left(-\frac{\zeta}{\gamma}\right) \tag{16}$$

The average probability or error can be given as:

$$P_e = \int_0^\infty Q\left(\frac{\mu_1(\zeta)-\mu_0}{\sigma_1(\zeta)+\sigma_0}\right)\frac{1}{\gamma}e^{-\frac{\zeta}{\gamma}} d\zeta \tag{17}$$

Making the change of variable $x^2 = \zeta/\gamma$ we then have

$$\begin{aligned} P_e &= 2\int_0^\infty x Q\left(\frac{\mu_1(\gamma x^2)-\mu_0}{\sigma_1(\gamma x^2)+\sigma_0}\right) e^{-x^2} dx\\ &= \int_{-\infty}^\infty |x| Q\left(\frac{\mu_1(\gamma x^2)-\mu_0}{\sigma_1(\gamma x^2)+\sigma_0}\right) e^{-x^2} dx \end{aligned} \tag{18}$$

Using the approximation

$$P_e \approx \sum_{i=-N;i\neq 0}^{N} w_i |x_i| Q\left(\frac{\mu_1(\gamma {x_i}^2) - \mu_0}{\sigma_1(\gamma {x_i}^2) + \sigma_0}\right) \quad (19)$$

IV. Numerical Results & Analysis

The average probability of error (11) has been calculated numerically to verify the closed-form approximation (15), as shown in Fig. 2.

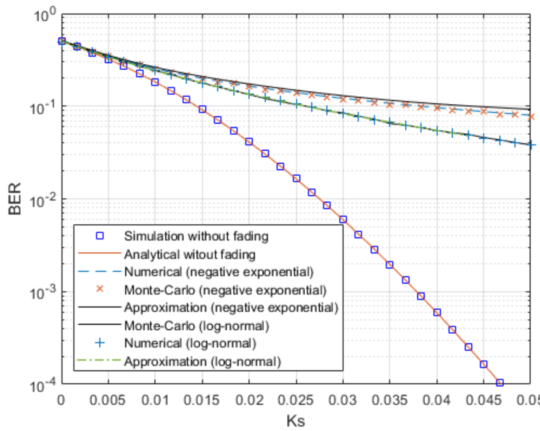

Fig. 2. BER results of SPAD array receiver (64x64) with and without fading channel (log-normal and negative exponential) for values of C_{FF} = 0.44 and K_{n} = 0.05 (T_{b} =1μs τ = 1ns).

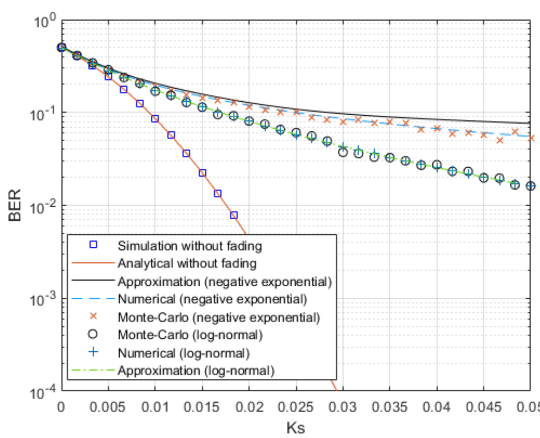

Fig. 3. BER results of SPAD array receiver (64x64) with and without fading channel (log-normal and negative exponential) for values of C_{FF} = 1 and K_{n} = 0.05 (T_{b} =1μs τ = 1ns).

The graph illustrates that the numerical integration is very close to the approximation expression, confirming the validity of the closed-form approximation. The graph depicts the difference in Bit Error Rate (BER) with and without fading channels (log-normal and negative exponential) and indicates an increase in BER when the channel fading is implemented. The Bit Error Rate (BER) is plotted as a function of K_{s} in this figure. However, the channel is effected by atmospheric turbulence. Furthermore, Monte-Carlo simulations perfectly match the curves of the numerical and approximation model results. Also, note that λ_{s} and λ_{n} must be known to optimally set the threshold, as the technical challenge with the On-Off Keying (OOK) system is used in this particular scenario. λ_{s} is a function of the channel fading that represents the transmission of "1" along with λ_{n}. The increase in the array Fill Factor (FF) improves the performance of the systems, meaning the array FF plays an important role in the SPAD-based receiver's performance.

Fig. 3 shows that the numerical integration is close to the approximation expression. The fading channel (log-normal and negative exponential) is implemented, resulting in an increased Bit Error Rate (BER) compared to the SPAD receiver implemented without a fading channel. It can be noted that in Fig. 3, the BER significantly reduces when the Fill Factor (FF) is increased compared to Fig. 2. However, Monte-Carlo simulation perfectly matches the curves of the approximation and the numerical model results. Furthermore, using the negative exponential channel model results in an increase in BER compared to the log-normal channel model along with the SPAD receiver.

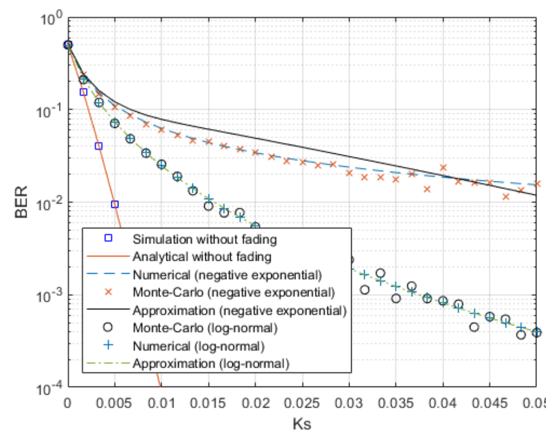

Fig. 4. BER results of SPAD array receiver (64x64) with and without fading channel (log-normal and negative exponential) for values of C_{FF} = 0.64 and K_{n} = 0.001 (T_{b} =1μs τ = 1ns).

Fig. 4 shows that the reduction in K_{n} significantly reduces the Bit Error Rate (BER), improving the performance of the systems along with an increase in the Fill Factor (FF), where K_{n} represents the noise.

V. Conclusion

In this paper, the analysis for the Single Photon Avalanche Diode (SPAD)-based free-space optical receiver was considered. A comprehensive analysis of the detection statistics for single SPAD and SPAD array receivers was discussed. Additionally, the effects of the fill factor and SPAD dead times on the Bit Error Rate (BER) performance were explored. The scenarios of atmospheric turbulence were modeled using both log-normal and negative exponential channel models in this work. Closed-form expressions for BER for both cases with SPAD detectors, considering the On-Off Keying (OOK) modulation scheme, were derived. Furthermore, the analytical results were compared with Monte-Carlo simulations, showing close agreement. Overall, an increase in BER with the rise in the scintillation index of atmospheric turbulence was observed.

REFERENCES

[1] M. A. Khalighi and M. Uysal, "Survey on free space optical communication: A communication theory perspective," *IEEE Communications Surveys Tutorials*, vol. 16, no. 4, pp. 2231–2258, 2014.

[2] X. Zhu and J. Kahn, "Free-space optical communication through atmospheric turbulence channels," *IEEE Transactions on Communications*, vol. 50, no. 8, pp. 1293–1300, 2002.

[3] X. Liu, "Free-space optics optimization models for building sway and atmospheric interference using variable wavelength," *IEEE Transactions on Communications*, vol. 57, no. 2, pp. 492–498, 2009.

[4] N. Faramarzpour, M. J. Deen, S. Shirani, and Q. Fang, "Fully integrated single photon avalanche diode detector in standard cmos 0.18- μm technology," *IEEE Transactions on Electron Devices*, vol. 55, no. 3, pp. 760–767, 2008.

[5] Y. Li, M. Safari, R. Henderson, and H. Haas, "Performance analysis of spad-based ofdm," *arXiv preprint arXiv:1905.06302*, 2019.

[6] J. H. Atkins and L. J. Gershell, "From the analyst's couch: Selective anticancer drugs," *Nature Reviews Drug Discovery*, vol. 1, no. 7, pp. 491–492, Jul 2002.

[7] E. Sarbazi, M. Safari, and H. Haas, "Photon detection characteristics and error performance of spad array optical receivers," in *2015 4th International Workshop on Optical Wireless Communications (IWOW)*, 2015, pp. 132–136.

[8] E. Sarbazi and H. Haas, "Detection statistics and error performance of spad-based optical receivers," in *2015 IEEE 26th Annual International Symposium on Personal, Indoor, and Mobile Radio Communications (PIMRC)*, 2015, pp. 830–834.

[9] K. Kiasaleh, "Performance of apd-based, ppm free-space optical communication systems in atmospheric turbulence," *IEEE Transactions on Communications*, vol. 53, no. 9, pp. 1455–1461, 2005.

[10] W. O. Popoola, Z. Ghassemlooy, and V. Ahmadi, "Performance of subcarrier modulated free-space optical communication link in negative exponential atmospheric turbulence environment," *International Journal of Autonomous and Adaptive Communications Systems*, vol. 1, no. 3, pp. 342–355, 2008.